Online Data Supplement

Inhibiting Lung Elastase Activity Enables Lung Growth In Mechanically Ventilated Newborn Mice

Anne Hilgendorff[1, 4], Kakoli Parai[1], Robert Ertsey[1], Noopur Jain[1], Edwin Navarro[1], Joanna Peterson[1], Rasa Tamosiuniene[2], Mark Nicolls[2], Barry Starcher[3], Marlene Rabinovitch[1], Richard Bland[1]

[1] Department of Pediatrics, Stanford University, Stanford, CA

[2] Department of Medicine, Stanford University, Stanford, CA

[3] Department of Biochemistry, University of Texas, Tyler, TX

[4] Department of Pediatrics, University of Munich, Munich, Germany

METHODS

Experimental design. This study was designed to determine if intrapulmonary treatment with the serine elastase inhibitor elafin would preserve matrix elastin and enable alveolar septation in lungs of newborn mice exposed to MV with 40%O_2 (MV-O_2) via tracheotomy for up to 24h. We previously reported the effects of prolonged MV-O_2 in disrupting lung elastin and inhibiting alveolarization in untreated 5d-old mice compared pto unventilated control pups that spontaneously breathed the same gas mixture (E1, E2). In this study our goal was to compare pulmonary responses to MV-O_2 in 5d-old mice that were pretreated, via tracheotomy, with either recombinant human elafin (40ng/g bw in 10μl/g bw) or vehicle alone (lactated Ringer's solution, L/R, 10μl/g bw), compared to unventilated controls that breathed 40%O_2 for up to 24h. In pilot studies, we found that pulmonary responses to MV-O_2 were virtually identical in 5d-old mice treated with intra-tracheal L/R when compared to untreated pups exposed to MV-O_2 for 24h (See results, **Figs E1-E6**).

We used full-term 5-6d old CD1 mice. The experimental approach was designed to avoid the severe lung injury that typically develops in response to MV with very high inflation pressures and extreme hyperoxia. We therefore used relatively modest tidal volumes (~7-8 μl/g body wt) and airway pressures (peak 13-20 cmH_2O, mean 4-6 cmH_2O), and limited the FiO_2 to 40%, thereby simulating the MV strategy that has been used to treat infants with respiratory failure. Such a ventilation strategy, using relatively low tidal volumes and peak inflation pressures, also has been applied to adults with ARDS, yielding less lung injury and improved survival (E3).

Mice randomly selected for MV had a tracheotomy under ketamine (~60 μg/g bw) and xylazine (~12 μg/g bw) anesthesia, as previously described (E2), followed by MV-O_2 at 180 breaths/min for 8h (to assess elastase and MMP-9 activity, lung expression of cytokines and chemokines, and NF-κKB-p65 nuclear protein content) or 24h (to assess all other endpoints) via a customized, small animal respirator (MicroVent model 848; Harvard Apparatus, Holliston, MA). Tidal volumes averaged 7-8μl/g bw and were similar for the groups that received MV. These ventilator settings were shown to yield a pH of 7.30 ± 0.12 and pCO_2 of 37 ± 11 mmHg in terminal samples of heart blood. Unventilated control mice had a midline neck incision under anesthesia (ketamine 75 μg, xylazine 15 μg), and then breathed 40%O_2 for 8h or 24h.

During MV mice were maintained in a neutral thermal environment and fed via an orogastric tube every 2h, initially with 10% glucose-0.25% saline solution, and later with milk formula, yielding a daily fluid intake of ~100-120 μL/g bw, as previously described (E2). Sedation with ketamine and xylazine (10 μg/g bw, and 2 μg/g bw, respectively) was repeated as needed. Urine was obtained by suprapubic needle aspiration when the bladder became visibly distended, and 24h urine collections were frozen for subsequent measurements of desmosine and creatinine concentrations. We measured heart rate and systolic blood pressure using a tail-cuff sensor device (BP Monitor Model MK-2000A, Muromachi Kikai Co., Tokyo) at the end of several studies. After 24h of MV-O_2, heart rate averaged 531 ± 50 beats/min and systolic blood pressure averaged 47 ± 8 mmHg, which are normal values for neonatal mice (E2). At the end of each study, pups were euthanized by injection of pentobarbital, ~150μg/g BW, for lung resection. Postmortem studies included measurement of lung elastase activity and MMP9 activity

in lung homogenates (8h studies); quantitative structural analyses and immuno-histochemistry (IHC) on fixed lung sections, immunoblot protein measurements on frozen lung specimens, and assays for desmosine and creatinine in urine (24h studies). All surgical and animal care procedures and experimental protocols were reviewed and approved by the Stanford University Institutional Animal Care and Use Committee.

Serine elastase activity in lung. Lung tissue was snap-frozen in liquid N_2 and stored at -80°C for measurement of serine elastase activity by a modification of a previously described method (E1, E4, E5) that uses DQ-elastin substrate (EnzChek® Elastase Assay Kit, Invitrogen, Camarillo, CA, cat no E12056). Activity was measured in the presence and absence of the serine proteinase inhibitor N-methoxysuccinyl-Ala-Ala-Pro-Val-chloromethyl ketone (0.01mmol). The selective serine elastase inhibitor elafin (5 µg/mL) was added to some samples, in lieu of the above inhibitor, before DQ-elastin.

MMP-9 activity in lung. Frozen lung samples were homogenized in PBS and electrophoresed onto 10% Tris-Glycine gel with 0.1% gelatin incorporated as a substrate (Invitrogen, Camarillo, CA, cat no EC61752BOX). SDS was removed from the gels by shaking in 2.5% Triton-X100 for one hour. The gels were then equilibrated in Zymogram Developing Buffer (Invitrogen, Camarillo, CA, USA) to add the divalent metal cation required for enzymatic activity. Elastolytic bands were visualized by Coomassie staining. Densitometric quantification of the protease bands was performed using a Gel Documentation System (BioRad, Hercules, CA), as previously described (E5).

RNA extraction and qRT-PCR for cytokines and chemokines*.* At the end of several 8h studies (n=4/group), lungs were excised and rapidly frozen in liquid N_2, then stored at -80°C for subsequent two-step mRNA extraction using Trizol reagent

(Invitrogen, Carlsbad, CA), and purification with RNeasy Mini Kit columns (Qiagen Inc, Valencia, CA). cDNA was synthesized from 2 μg of total purified RNA using reverse transcriptase (SuperScript III kit, Invitrogen). Amplification was performed in triplicate at 50°C for 2 min, 95°C for 10 min, followed by 40 cycles at 95°C for 15 sec and 60°C for 1 min. Reactions without template were used as negative controls. 18S ribosomal RNA was used as an internal control. Standard curves were plotted for each target gene and internal control. RNA quantity was expressed relative to the corresponding 18S ribosomal RNA control. Primers and probes for target genes and controls were obtained from Applied Biosystems (TaqMan Gene Expression Assays, Applied Biosystems Inc, Foster City, CA) and analyzed on a CFX384 Real Time thermal cycler (Bio-Rad Laboratories, Hercules, CA). ΔΔCt analysis was used to determine the expression level of each gene normalized to 18S using CFX384 analysis software (Bio-Rad). Specific genes that were measured by qRT-PCR included interleukin-1β (IL-1β), IP-10 interferon-γ inducible protein-10 (IP-10; aka CXCL10), monocyte colony stimulating factor (M-CSF), tumor necrosis factor-α (TNF-α), macrophage inflammatory protein-2 (MIP-2; aka CXCL2), monocyte chemotactic protein-1 (MCP-1; aka CCL2), and RANTES (regulated upon activation, normal T-cell expressed and secreted; aka CCL5).

Postmortem processing of lungs for quantitative histology. To process lungs for histopathology (n=5-6/group), the diaphragm was punctured via the abdomen to permit lung expansion during instillation of fixative via the tracheotomy tube. For unventilated control pups, a tracheotomy and diaphragm opening were made after a lethal injection of pentobarbital. The lungs were fixed intra-tracheally with buffered 4% PFA (pH=7.4) at an inflation pressure of 20 cmH_2O overnight at 4°C, as previously described (E2). The

fixed lungs were excised, their volume measured by fluid displacement (E6), and they were embedded in paraffin for isotropic uniform random (IUR) sectioning. Tissue sections (4 μm) were stained with hematoxylin and eosin for quantitative assessment of alveolar diameter and area using the Bioquant image analysis system (R & M Biometrics, Nashville, TN) (E2); alveolar number was determined by radial alveolar counts, as previously described (E7).

Postmortem lung morphometry. Isotropic uniform random (IUR) orientation of the lungs was achieved by cutting the paraffin blocks at random angles in two perpendicular planes. Random angles were selected using a random number chart, and were applied using an orientator (E8). The IUR paraffin blocks were then transferred onto mounting blocks for sectioning. A random number generator was used to determine a number from 1 to 90, defining how many μm from the leading edge of lung tissue serial sectioning would begin. A series of 12 4μm sections was generated every 360μm. Lung sections were stained with hematoxylin and eosin for structural analysis, and with Hart's stain for assessing lung content and distribution of elastin.

To determine the size and number of alveoli in lungs of mice from each of the groups, we measured alveolar area and diameter, and radial alveolar counts (RAC), respectively. Four slides per animal were randomly selected using a random number table. Using a Nikon Eclipse E800 microscope and Bioquant Osteo II MIR software (Bioquant Osteo version 8.00.20 BQXI, Nashville, TN), the area of all complete alveoli (non-branching, terminal airspaces with complete alveolar walls) was measured using a 20X objective (200X magnification) in 3 fields of view per slide. For smaller lung sections that had fewer than 3 fields of view, an additional lung section was used to

obtain a total of 12 fields per mouse. Regions of atelectasis or lung collapse, in which alveolar walls were folded, were not counted. Non-overlapping counts were guaranteed by marking each individual alveolus as it was measured, such that overlapping fields of view were avoided. Alveolar area measurements obtained on the lungs of each mouse were combined, and their respective means calculated. Analyses were done without knowledge of the group from which the lung sections derived.

Alveolar number across terminal respiratory units was estimated by assessing RAC according the method described by Emery and Mithal (E7), modified for optimal accuracy according to the recommendations of Cooney and Thurlbeck (E9). Briefly, a line was drawn from the center of the terminal respiratory unit to the nearest septum or pleura. The number of alveolar spaces crossed by the line was determined, and the average number of alveoli per terminal respiratory unit was calculated, yielding the RAC for each mouse. Four slides per mouse were selected using a random number table. All terminal respiratory units were assessed on each tissue section viewed through a 10X objective (100X magnification).

Quantitative image analysis of insoluble cross-linked elastin. Measurement of insoluble cross-linked elastin in lung was performed using the Bioquant Osteo II MIR software and Nikon Eclipse E800 microscope. Four slides per mouse were randomly selected, and 12 fields of view per mouse were assessed through a 40X objective (400X magnification). To measure lung elastin content, automated video “thresholding” of stain color was performed using the Bioquant True Color Windows Image Analysis system (R & M Biometrics, Nashville, TN), as previously described (E1). Elastin stain

surface area was expressed as a percentage of counter-stained lung tissue surface area to reflect the relative lung abundance of cross-linked elastic fibers.

Immunohistochemistry for recombinant human elafin. To verify that the elafin dose that was delivered via tracheotomy was distributed uniformly throughout the lungs, we randomly selected PFA-fixed lung sections from each of the 24h study groups (n=2-4/group) for IHC using methods similar to those described in the main manuscript. Briefly, deparafifinized tissue sections were pre-treated for antigen retrieval (Dako, Carpenteria, CA), followed by blocking serum and application of the primary antibody (rabbit anti-elafin, 1:100, Santa Cruz, sc-20637) overnight at 4°C. Immune complexes were visualized with the relevant peroxidase-coupled secondary antibody using the Vectastain kit (Vector Laboratories, Burlingame, CA).

Protein extraction and immunoblots. To measure lung abundance of cleaved caspase-3 protein, frozen lung tissues were homogenized at 4°C in a solution containing 50 mM Tris-HCl, pH=7.5, 20 mM CHAPS, 3 mM DTT and Halt^{TM} protease inhibitor cocktail (Pierce Biotechnology Inc, Rockford, IL). Homogenate samples were mixed at 4°C for 60min on a rocker platform, centrifuged at 14,000g for 30min, and supernatants were stored at -80°C. Protein concentration was measured in aliquots of tissue extracts using the DC Protein Assay Kit (Bio-Rad Laboratories, Hercules, CA). Proteins were separated on SDS-PAGE gels (Invitrogen Life Technologies, Carlsbad, CA) and blotted electrophoretically onto 0.45-μm nitrocellulose membranes (Invitrogen). Membranes were blocked with a solution of 5% non-fat milk in TBS buffer containing 0.05% Tween-20 at room temperature for 1h. Membranes were incubated with specific

primary antibodies, diluted in a solution of 5% non-fat milk in TBS buffer containing 0.05% Tween-20 under specific conditions, as described below.

Immunoblot analysis was applied to measure cleaved caspase-3 protein using a 1:250 dilution of rabbit monoclonal antibody (catalog number 9664, Cell Signaling Technologies, Danvers, MA). Antibody-coated membranes were incubated overnight at 4°C. Membranes then were washed 3 times in a solution containing 0.05% Tween-20 and TBS buffer, after which the membranes were incubated at room temperature for 1h with a dilute (1:5000) solution of a secondary antibody (goat anti-rabbit IgG; sc-2301, Santa Cruz) conjugated to horseradish peroxidase, followed by 3 washes. Images were detected by chemiluminescence (ECL or ECL+ Detection Kit, Amersham Life Science Inc, Piscataway, NJ) and quantified by densitometry using a Gel Documentation System (Bio-Rad, Hercules, CA). Membranes were stripped and re-probed with a 1:5,000 dilution of rabbit polyclonal anti-β-actin antibody (ab-8227, Abcam Ltd. Cambridge, MA) and incubated at room temperature for 1h to provide an internal loading control.

Nuclear extracts and immunoblots for NF-κB-p65. Some lungs that were excised at the end of 24h were snap-frozen in liquid N2 and stored at -80°C for later extraction of nuclear cell fractions and immunoblot analysis of p65 as an index of NF-ΚB activation. Harvested lung tissue was pretreated with protease inhibitor (Pierce Biotech, Rockford, IL, cat #78410) and homogenized in ice cold collection buffer that was provided in a nuclear protein extraction kit (NE-Per Kit, Pierce Biotech, cat #78833). Nuclear extracts, obtained according to the manufacturer's instructions, were incubated overnight with NF-κB-p65 primary antibody (1:700, Santa Cruz Biotech, cat #sc-372).

ELISA for lung TGFβ activity. Lung tissue samples (20-30 mg) were homogenized in PBS with added protease inhibitor (Pierce) and centrifuged at 14000 rpm for 30 min at 4°C. Supernatants were collected, and protein concentration was determined by the Bradford assay (Bio-Rad). Equal amounts of protein from each sample were loaded for analysis of TGFβ1 activity using an ELISA kit (MB100B, R&D Systems, Minneapolis, MN) according to the manufacturer's instructions. All samples were analyzed in duplicate as a single batch, and run with control standards. Total TGFβ1 was measured by activating latent TGFβ with acidification using 1N HCl, followed by neutralization with 1.2N NaOH/0.5M HEPES. Active and total TGFβ samples were pipetted separately onto the precoated ELISA plate and sandwiched with TGFβ1 conjugate antibody, yielding a colorimetric reaction from which optical density was determined at 450 and 570 nm. The ELISA detection range for the assay is 5-2000 pg/ml. There is no cross reactivity with other forms of TGFβ or any of the bone morphogenic proteins, as documented by the manufacturer.

RESULTS

Preliminary control studies. We did preliminary studies to compare the effects of MV-O_2 for 24h on the lungs of 5d-old untreated CD1 mice vs L/R-treated pups in order to determine that the vehicle in which elafin was delivered had no discernible beneficial or adverse pulmonary effects that might have obscured interpretation of our results. We found that the pulmonary response to 24h of MV-O_2, with respect to all of the variables that we assessed, was virtually identical in mice that were treated with intrapulmonary

L/R vs untreated mice (**Figs E1-E6**). Likewise, results obtained for the L/R-treated mice were similar to those previously reported for 5d-old untreated Balb/c mice that had MV-O_2 for 24h (E1, E2).

Lung distribution of recombinant human elafin. **Fig E7** shows that elafin was uniformly distributed throughout the distal lung, in sharp contrast to the vehicle-treated lung that was free of stain. Multiple tissue sections showed that the instilled elafin distributed equally throughout all lung lobes, with no detectable unstained regions.

Lung mRNA expression of pro-inflammatory cytokines. Elafin treatment fully suppressed the increased expression of IL-1β and IP-10 (CXCL10) noted in lungs of vehicle-treated pups after MV-O_2 for 8h, and also reduced levels of TNF-α and MCP-1 below levels of control and vehicle-treated pups (**Fig E8**). There was a trend toward increased lung expression of M-CSF mRNA after MV-O_2 in L/R-treated mice (p=0.1), which was suppressed by elafin treatment. mRNA expression of MIP-2 and RANTES increased in response to MV-O_2, an effect that elafin did not inhibit. The MV-O_2 related increase of MIP-2 expression was accentuated in the lungs of pups that received elafin treatment.

Lung content of NF-κB-p65 protein. As elafin has been reported to suppress activation of transcription factor NF-κB in endothelial cells and macrophages exposed to endotoxin and other atherogenic stimuli (E10), we measured lung content of p65 protein, a subunit of the NF-κB transcription factor complex, which plays a key role in inflammatory and immune responses. Elafin treatment markedly suppressed lung content of p65 after 8h of MV-O_2 compared to unventilated controls and vehicle-treated pups (**Fig E9**). Lung p65 protein, however, did not increase in vehicle-treated pups that

received MV-O_2, suggesting that NF-KB activation was unlikely a direct cause of the lung pathology observed in this group.

Active TGFβ in whole lung homogenates. To complement immunohistochemical assessment of pSmad-2 in peripheral lung as an index of TGFβ activation, which elafin inhibited during MV-O_2, we used an ELISA assay to measure active TGFβ in whole lung homogenates obtained from the three groups of mice. While the results were consistent with a suppressive effect of elafin on TGFβ signaling (**Fig E10**), the apparent differences in TGFβ activity between elafin-treated and control groups did not reach statistical significance (p=.08), perhaps related to small sample size (n=4/group), considerable variability in the control and vehicle-treated groups, and regional differences in TGFβ activity that may be obscured by measurements made on protein extracts of whole lung tissue.

SUPPLEMENT FIGURES

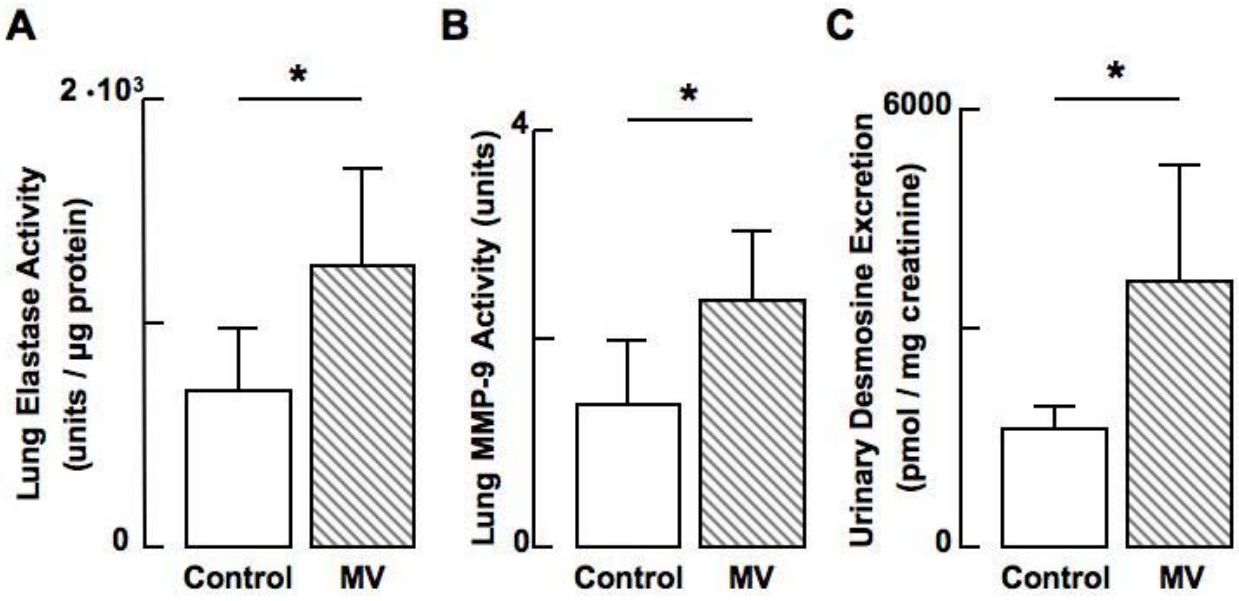

Fig E1. MV-O_2 for 8h increases **(A)** serine elastase activity, and **(B)** MMP-9 activity in lungs of 5d old untreated mice (hatched bar) that received neither L/R nor elafin, compared with unventilated, untreated control mice (white bar). n=3-4/group. **(C)** MV-O_2 for 24h increased urinary excretion of desmosine, a marker of elastin degradation, in 5-6d old untreated mice (hatched bar), compared with unventilated, untreated mice (white bar). n=10-12/group. Mean & SD. *****Significant difference, $p < 0.05$.

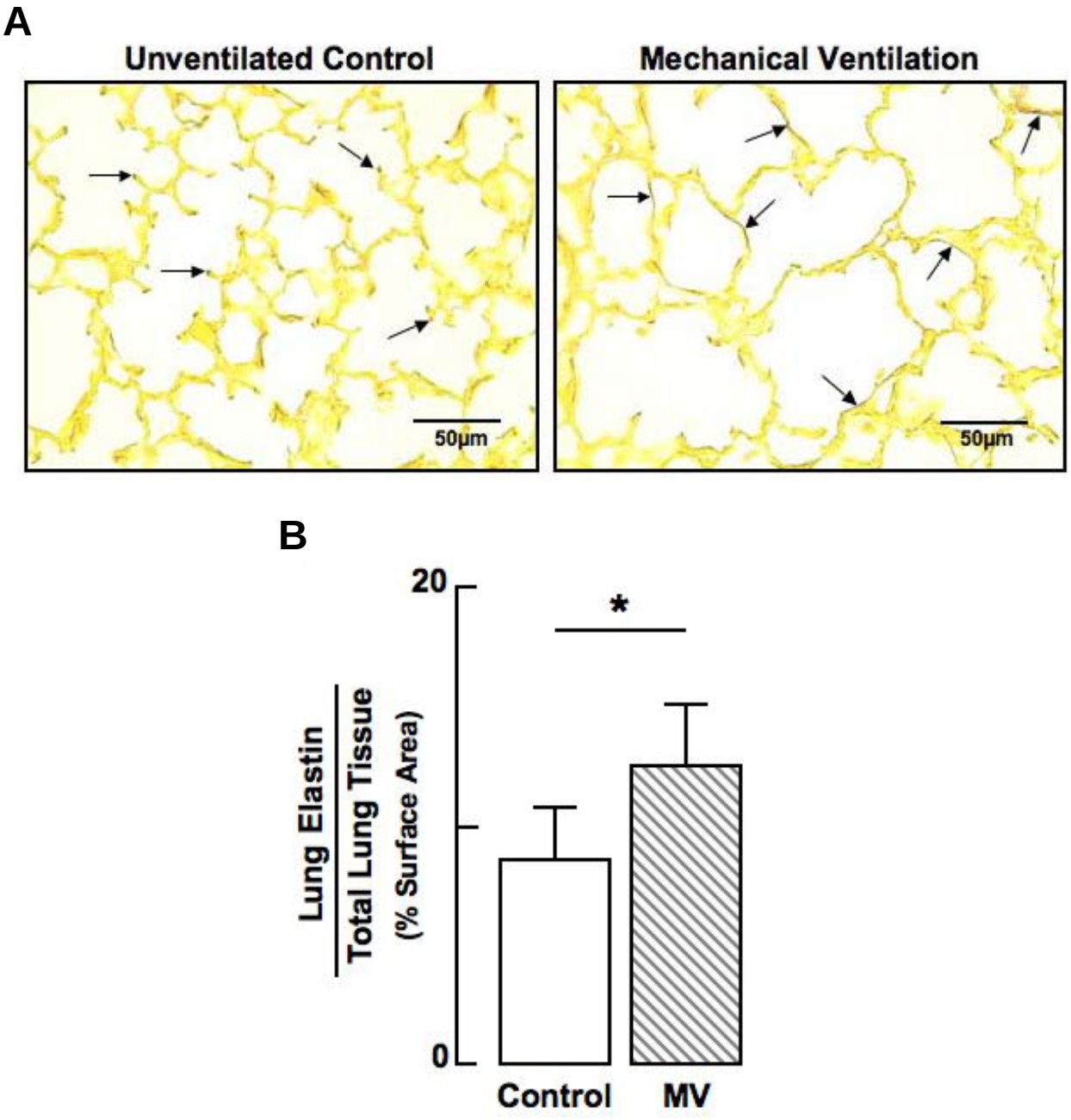

Fig E2. MV-O_2 for 24h results in widely dispersed lung elastin. **(A)** Lung sections stained for elastin (Hart's stain), showing elastin mainly at the septal tips (arrows) in the unventilated control lung, vs maldistributed elastic fibers scattered throughout the walls of distal airspaces in the untreated lung (that received neither L/R nor elafin) exposed to MV-O_2 for 24h. **(B)** Summary data showing that MV-O_2 for 24h increased elastin in untreated lungs (hatched bar) compared with unventilated control lungs (white bar). Mean & SD. n=4-5/group. *****Significant difference, $p < 0.05$.

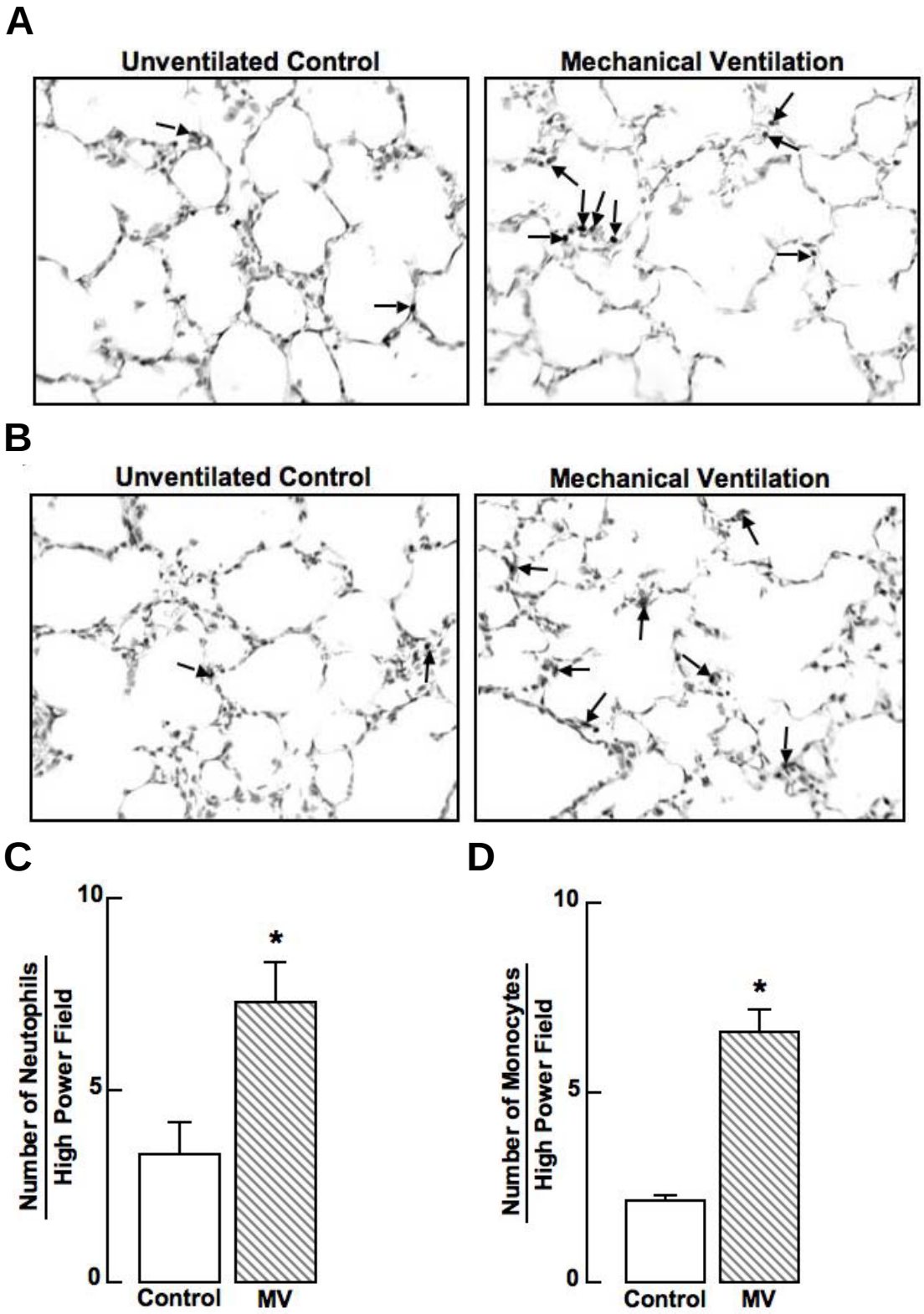

Fig E3. MV-O_2 for 24h induces inflammation in lungs of newborn mice. IHC for **(A)** neutrophils (arrows) and **(B)** monocytes (arrows) in lung sections of an unventilated 6d-old control mouse that breathed 40% O_2 for 24h compared with an untreated pup that had MV-O_2 for 24h. Magnification 400X. Summary data showing that MV-O_2 increased lung influx of both neutrophils **(C)** and monocytes **(D)** in mice treated with neither L/R nor elafin. Mean & SD. n=4/group. *****Significant difference, $p < 0.05$.

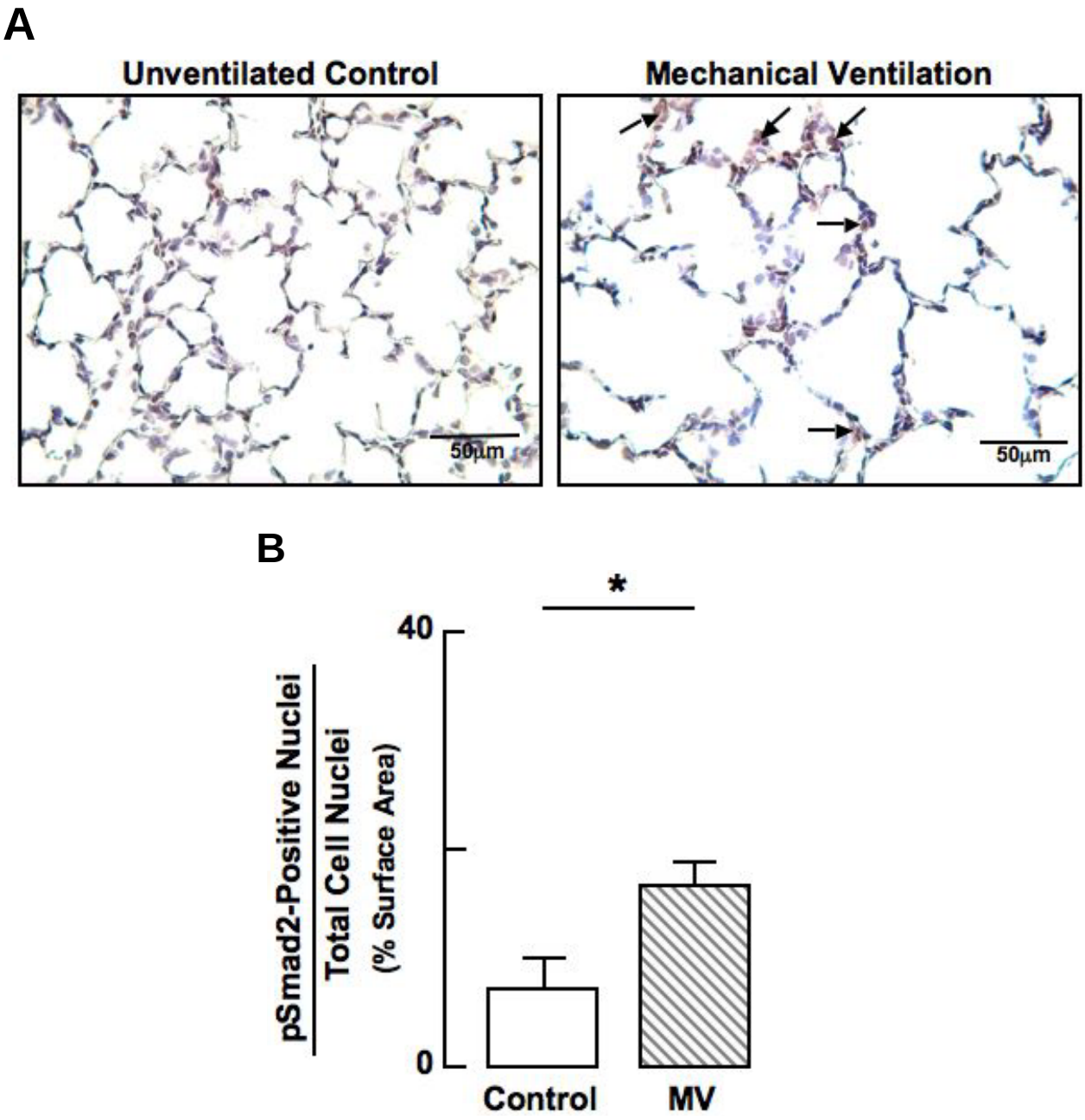

Fig E4. MV-O_2 for 24h increases TGFβ signaling in lungs of newborn mice. **(A)** IHC for pSmad-2 protein in PFA-fixed lung sections of 6d-old mice showing increased nuclear staining (arrows), indicative of TGFβ activation, in the lung exposed to MV-O_2 for 24h compared with the lung of an unventilated control pup that breathed 40%O_2 for 24h. **(B)** Summary data showing that MV-O_2 for 24h caused a >2-fold increase of pSmad-2 expressing cells in lungs of untreated mice (hatched bar) compared with unventilated control mice (white bar). Mean & SD. n=4-7/group. *****Significant difference, $p < 0.05$.

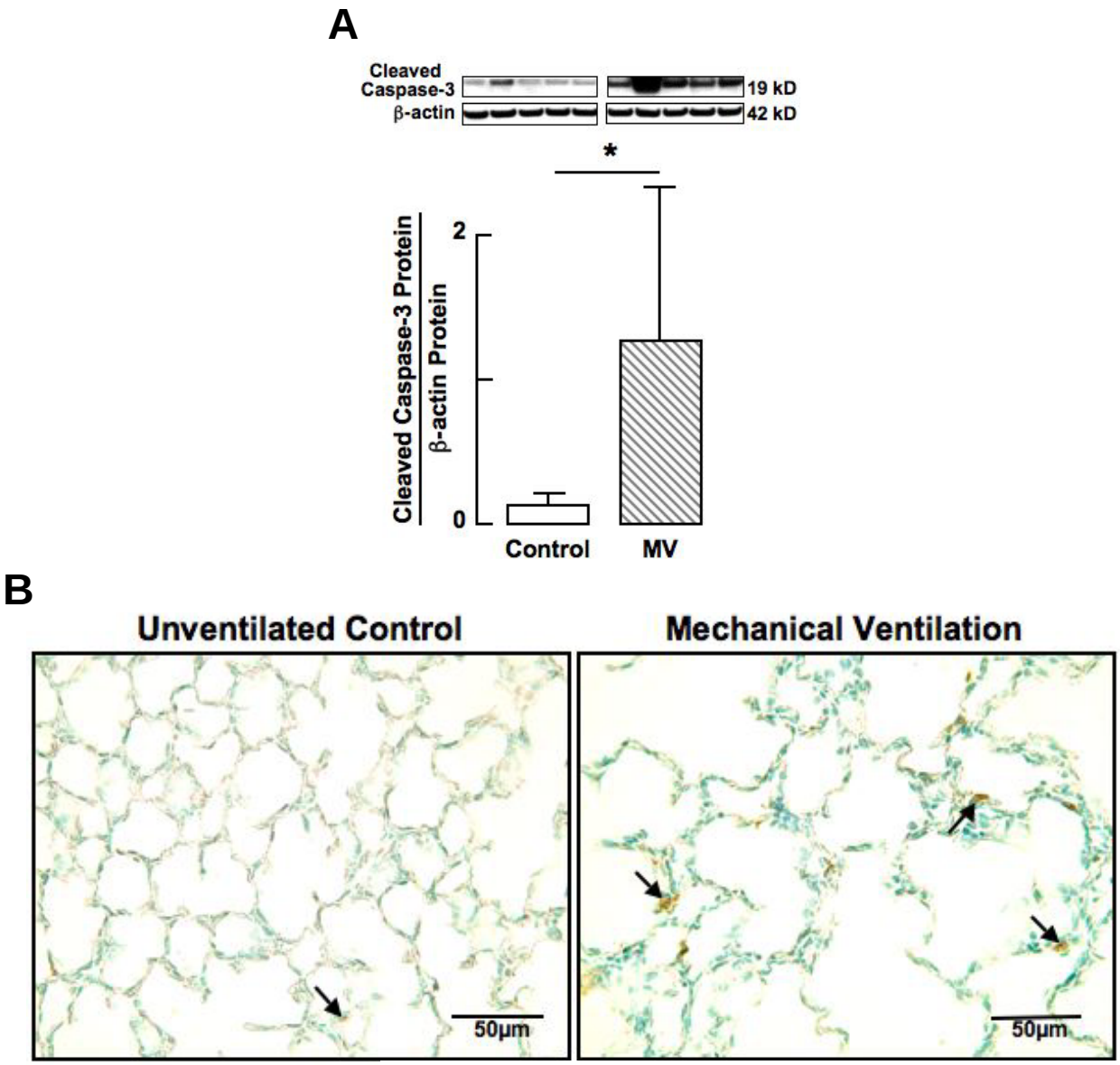

Fig E5. MV-O_2 for 24h increases apoptosis in newborn mice. **(A)** Immunoblots of cleaved caspase-3 protein showing a ~10-fold increase in lungs of 6d-old mice exposed to MV-O_2 for 24h (hatched bar), compared with unventilated controls (white bar). **(B)** TUNEL-stained lung sections showing abundant apoptotic cells (arrows) after MV-O_2 for 24h in the untreated (neither L/R nor Elafin) lung compared with the lung from an unventilated, untreated mouse pup. Magnification 400X. **(C)** Summary data showing a 3-fold increase in TUNEL-stained cell nuclei relative to total cell nuclei in mice that had MV-O_2 for 24h (hatched bar), compared with unventilated pups that breathed 40%O_2 for 24h (white bar).
Mean&SD. n=4-5/group. *****Significant difference, p<.05.

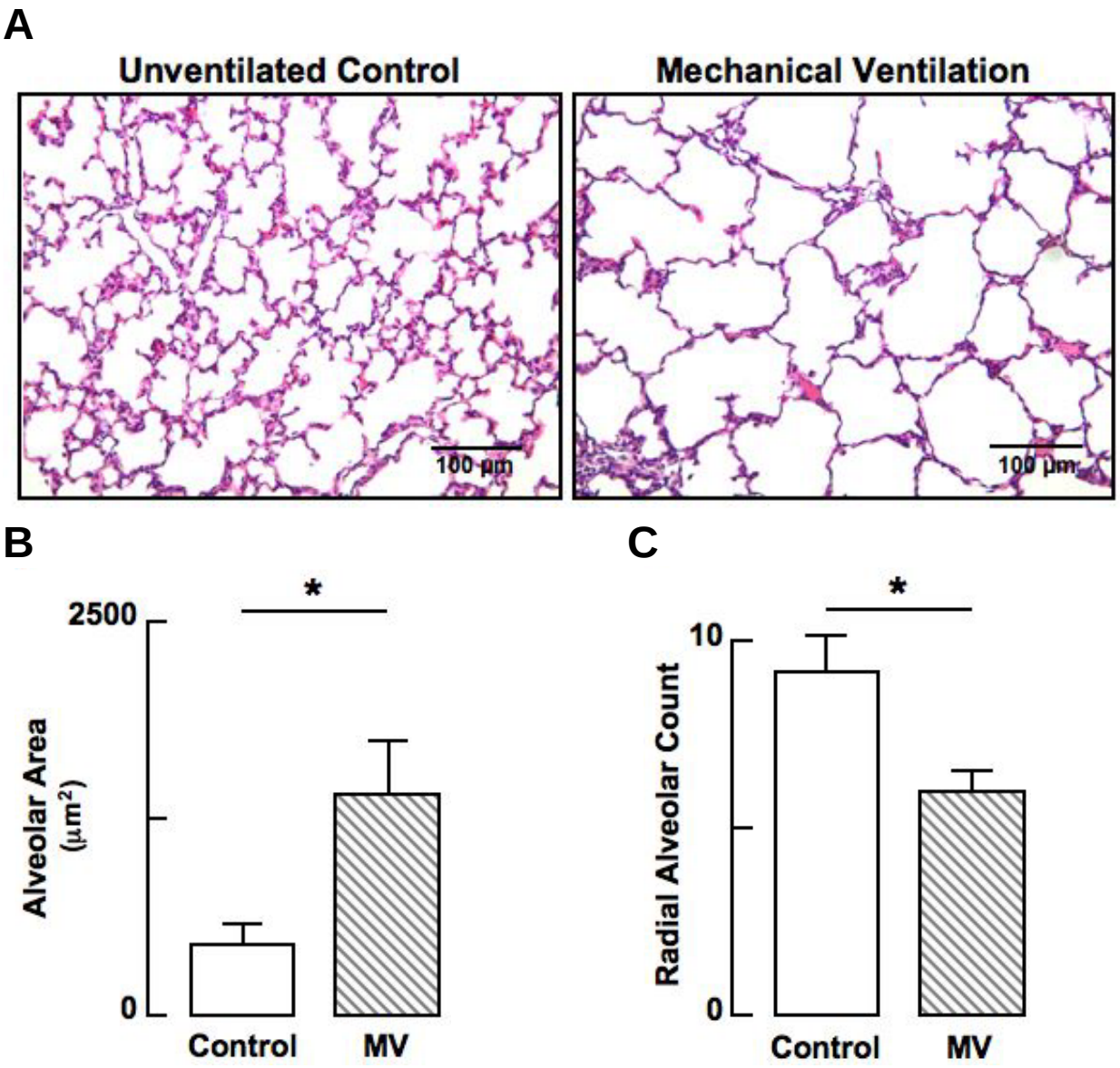

Fig E6. MV-O_2 for 24h impairs alveolar septation, resulting in larger and fewer alveoli in lungs of newborn mice. **(A)** Lung sections showing reduced alveolar septation and larger alveoli in lungs of untreated (neither L/R nor elafin treatment) 6d-old mice compared with unventilated, untreated control mice. Magnification 200X.
(B) Summary data showing that MV-O_2 caused a 3- to 4-fold increase in alveolar size in untreated mice (hatched bar) compared with unventilated control mice (white bar).
(C) Summary data showing that MV-O_2 caused a ~40% decrease in radial alveolar count, an index of alveolar number, in lungs of untreated mice (hatched bar) compared with unventilated control mice (white bar).
Mean&SD. n=5-7/group. *****Significant difference, p<.05.

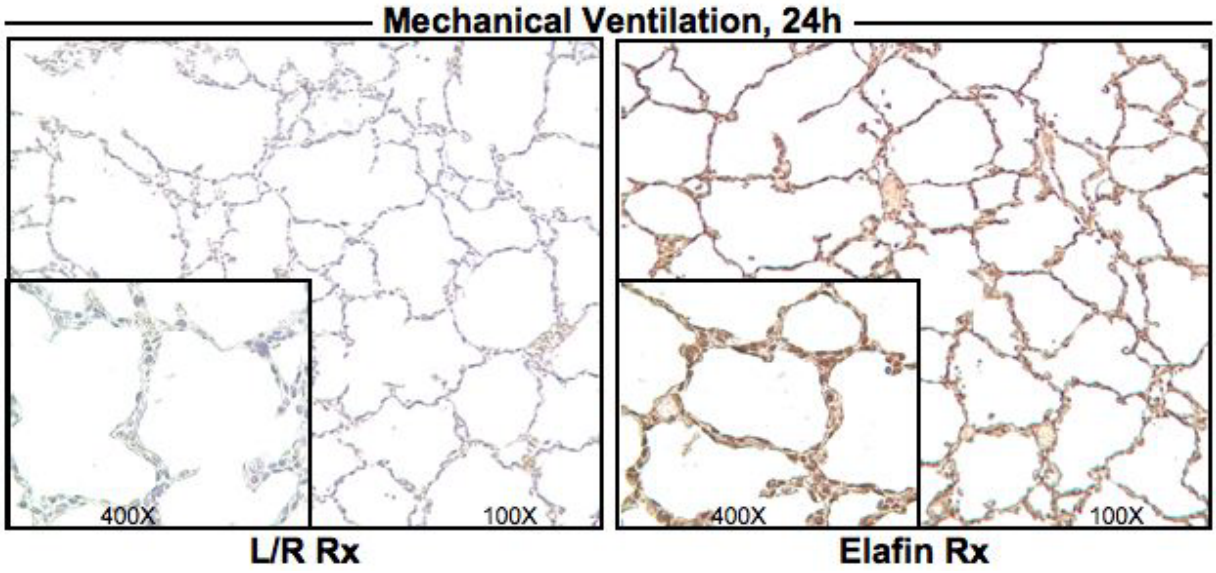

Fig E7. IHC staining for recombinant human elafin (brown stain) in lung tissue sections obtained from 6d-old mice that received MV-O_2 for 24h after intra-tracheal treatment with L/R (left panel) or elafin (right panel), showing uniform distribution of elafin 24h after treatment. Larger images shown at 100X, inserts shown at 400X magnification.

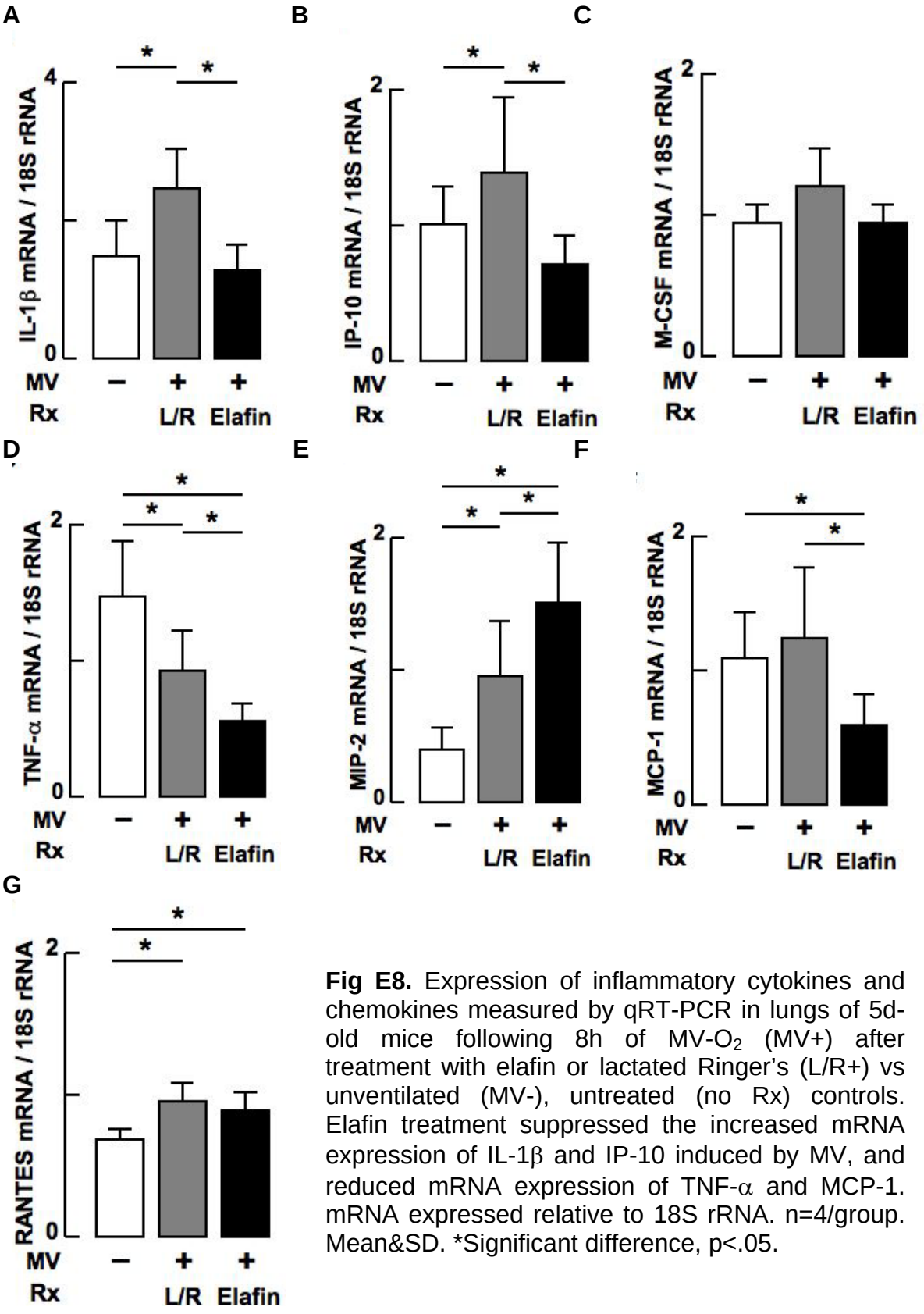

Fig E8. Expression of inflammatory cytokines and chemokines measured by qRT-PCR in lungs of 5d-old mice following 8h of MV-O_2 (MV+) after treatment with elafin or lactated Ringer's (L/R+) vs unventilated (MV-), untreated (no Rx) controls. Elafin treatment suppressed the increased mRNA expression of IL-1β and IP-10 induced by MV, and reduced mRNA expression of TNF-α and MCP-1. mRNA expressed relative to 18S rRNA. n=4/group. Mean&SD. *Significant difference, p<.05.

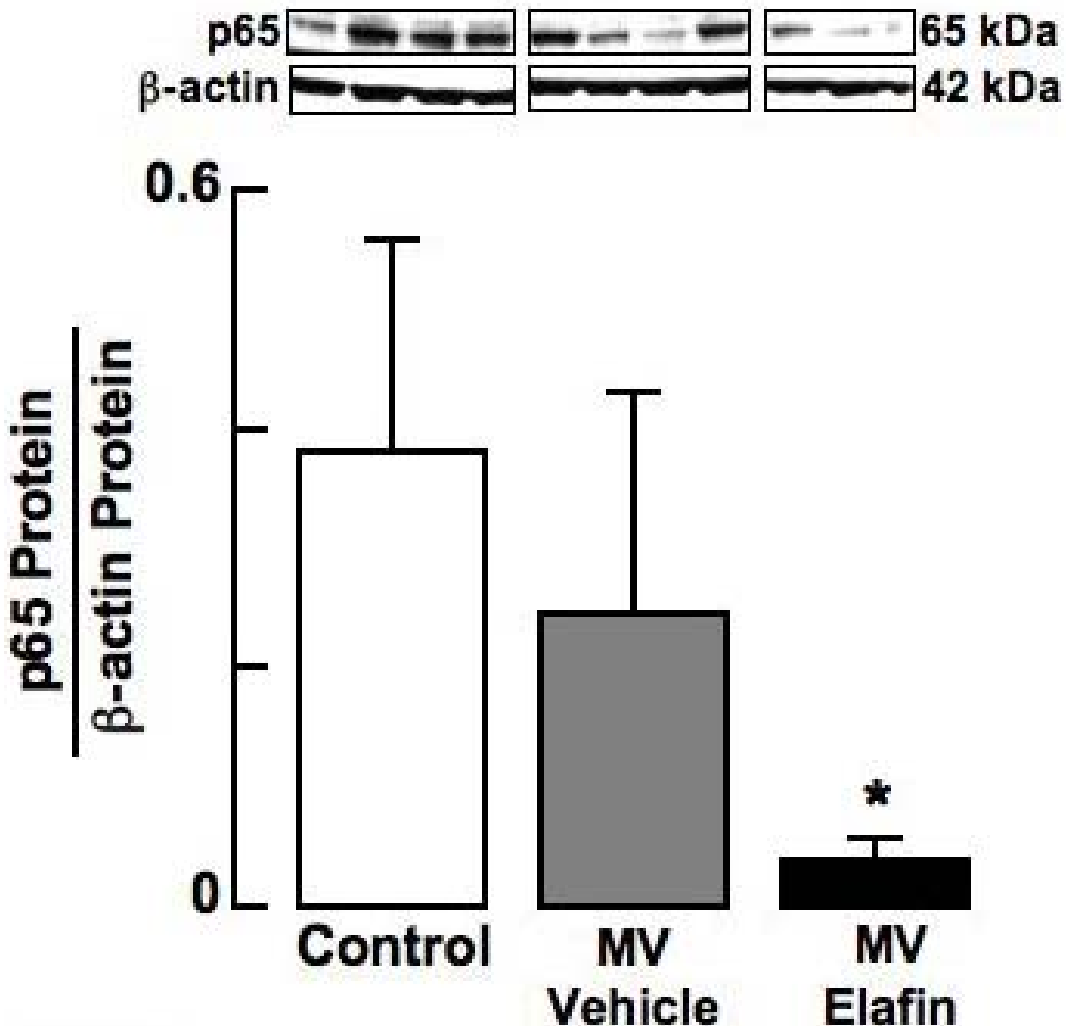

Fig E9. Immunoblots showing reduced abundance of NF-KB-p65 in nuclear extracts of lungs obtained from 5d-old mice that received MV-O_2 for 8h after treatment with elafin compared with mice that received vehicle (L/R). Control mice received neither MV-O_2 nor treatment with elafin or L/R. Note that p65 protein did not increase in response to MV in L/R-treated mice, suggesting that NF-KB activation was not the primary cause of the lung pathology seen after MV-O_2. n=3-4/group. Mean&SD. *Significant difference vs Control group, p<.05.

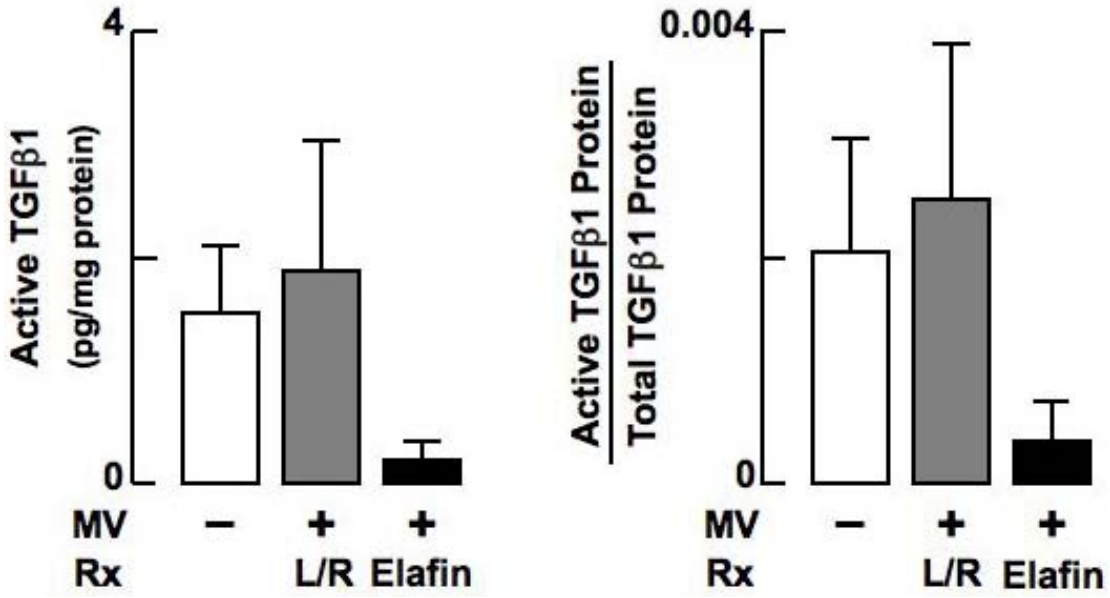

Fig E10. Active TGFβ1, measured by ELISA, in total lung homogenates of 6d-old mice following MV-O_2 (MV+) for 24h after treatment with either elafin (Elafin+) or lactated Ringer's solution (L/R+), compared with unventilated (MV-), untreated (no Rx) pups. Note the low level of active TGFβ1 in the lungs of elafin-treated mice. Owing to large variability and small sample size (n=4/group), however, apparent differences between elafin-treated and control groups were not statistically significant (p=0.08). The pattern was similar between groups for the ratio of active TGFβ1/total TGFβ1 protein. Mean&SEM.

SUPPLEMENT REFERENCES

E1. Bland RD, Ertsey R, Mokres LM, Xu L, Jacobson BE, Jiang S, Alvira CM, Rabinovitch M, Shinwell, ES, Dixit A. Mechanical Ventilation Uncouples Synthesis and Assembly of Elastin and Increases Apoptosis in Lungs of Newborn Mice. *Am J Physiol Lung Cel Mol Physiol.* 2008; 294:L3-L14.

E2. Bland RD, Mokres LM, Ertsey R, Jacobson BE, Jiang S, Rabinovitch M, Xu L, Shinwell ES, Zhang F, Beasley MA. Mechanical Ventilation with 40% Oxygen Reduces Pulmonary Expression of Genes That Regulate Lung Development and Impairs Alveolar Septation in Newborn Mice. *Am J Physiol Lung Cell Mol Physiol.* 2007; 293:L1099-L1110.

E3. The Acute Respiratory Distress Syndrome Network. Ventilation with lower tidal volumes as compared with traditional tidal volumes for acute lung injury and the acute respiratory distress syndrome. *New Engl J Med.* 2000; 342:1301-1308.

E4. Bland RD, Xu L, Ertsey R, Rabinovitch M, Albertine KH, Wynn KA, Kumar VH, Ryan RM, Swartz DD, Csiszar K, Fong K. Dysregulation of pulmonary elastin synthesis and assembly in preterm lambs with chronic lung disease. *Am J Physiol Lung Cell Mol Physiol.* 2007; 292:L1370-L1384.

E5. Zaidi SH, You XM, Ciura S, Husain M, Rabinovitch M. Overexpression of the serine elastase inhibitor elafin protects transgenic mice from hypoxic pulmonary hypertension. *Circulation.* 2002; 105:516-521.

E6. Scherle W. A simple method for volumetry of organs in quantitative stereology. *Mikroskopie.* 1970; 26:57-60.

E7. Emery JL, Mithal A. The number of alveoli in the terminal respiratory unit of man during late intrauterine life and childhood. *Arch Dis Child.* 1960; 35:544-547.

E8. Hyde DM, Tyler NK, Putney LF, Singh P, Gundersen HJ. Total number and mean size of alveoli in mammalian lung estimated using fractionator sampling and unbiased estimates of the Euler characteristic of alveolar openings. *Anat Rec A Discov Mol Cell Evol Biol.* 2004; 277:216-226.

E9. Cooney TP, Thurlbeck WM. The radial alveolar count method of Emery and Mithal: a reappraisal 1--postnatal lung growth. *Thorax.* 1982; 37:572-579.

E10. Henriksen PA, Hitt M, Xing Z, Wang J, Haslett C, Riemersma RA, Webb DJ, Kotelevtsev YV, Sallenave J-M. Adenoviral gene delivery of elafin and secretory leukocyte protease inhibitor attenuates NF-KB-dependent inflammatory responses of human endothelial cells and macrophages to atherogenic stimuli. *J Immunol.* 2004; 172:4535-4544.